

1      Supplementary Information for:

2      **Multiscale 3D microfluidic platform for intraorganoid delivery**

3      **Author List:** Maria Jose Quezada<sup>1,2,3†</sup>, Jamin Lee<sup>1,4,5,6†</sup>, Zengyao Lv<sup>7†</sup>, Khizar Nandoliya<sup>8†</sup>, Ingrid  
4      Cheung<sup>1,9†</sup>, Qiong Wang<sup>6,†</sup>, Woo-Yeol Maeng<sup>6</sup>, Naijia Liu<sup>6</sup>, Amir Vahabikashi<sup>10</sup>, Kyoung-Ho Ha<sup>6</sup>,  
5      Yong-Woo Kang<sup>6</sup>, Dae-Hyeon Song<sup>11</sup>, Yuming Huang<sup>6</sup>, Clara Asseily<sup>2</sup>, Rakan Walid da Cruz<sup>2</sup>,  
6      Shreyaa Khanna<sup>1</sup>, Jintao Liu<sup>12,13</sup>, John D. Finan<sup>14</sup>, Lara Leoni<sup>15</sup>, Daniele Prociassi<sup>15</sup>, Yonggang  
7      Huang<sup>6,7,16</sup>, Gyu-Chul Yi<sup>4,5</sup>, Juyeol Bae<sup>12,13\*</sup>, John A. Rogers<sup>2,6,16\*</sup> & Colin K. Franz<sup>1,6,9,17\*</sup>

8

9      **Affiliations:**

10     <sup>1</sup>Regenerative Neurorehabilitation Laboratory, Shirley Ryan Ability Lab, Chicago, IL 60611,  
11     USA.

12     <sup>2</sup>Department of Biomedical Engineering, Northwestern University, Evanston, IL 60208, USA.

13     <sup>3</sup>Department of Physical Therapy and Human Movement Sciences, Northwestern University,  
14     Chicago, IL 60611, USA.

15     <sup>4</sup>Interdisciplinary Program in Neuroscience, College of Science, Seoul National University, Seoul,  
16     08826, South Korea.

17     <sup>5</sup>Center for Novel Epitaxial Quantum Architectures, Department of Physics and Astronomy, Seoul  
18     National University, Seoul, 08826, South Korea.

19     <sup>6</sup>Querrey Simpson Institute for Bioelectronics, Northwestern University, Evanston, IL, 60208,  
20     USA.

21     <sup>7</sup>Department of Civil and Environmental Engineering, Northwestern University, Evanston, IL  
22     60208, USA.

23     <sup>8</sup>Department of Neurological Surgery, Feinberg School of Medicine, Northwestern University,  
24     Chicago, IL 60611, USA.

25     <sup>9</sup>Department of Physical Medicine and Rehabilitation, Northwestern University.

26     <sup>10</sup>Bioengineering Department and Institute for Mechanobiology, Northeastern University, Boston,  
27     MA, 02115, USA.

28     <sup>11</sup>Department of Materials Science and Engineering, Korea Advanced Institute of Science and  
29     Technology, Daejeon, 34141, South Korea.

30     <sup>12</sup>Department of Mechanical Engineering, Chonnam National University, 77 Yongbong-ro, Buk-  
31     gu, Gwangju 61186, Republic of Korea.

32 <sup>13</sup>Advanced Medical Device Research Center for Cardiovascular Disease, Chonnam National  
33 University, 77 Yongbong-ro, Buk-gu, Gwangju 61186, Republic of Korea

34 <sup>14</sup>Department of Mechanical and Industrial Engineering, University of Illinois Chicago, Chicago,  
35 IL 60607, USA.

36 <sup>15</sup>Department of Radiology, Feinberg School of Medicine, Northwestern University, Chicago, IL  
37 60611, USA.

38 <sup>16</sup>Department of Materials Science and Engineering and Department of Mechanical Engineering,  
39 Northwestern University, Evanston, IL 60208, USA.

40 <sup>17</sup>The Ken and Ruth Davee Department of Neurology, Feinberg School of Medicine, Northwestern  
41 University, Chicago, IL 60611, USA.

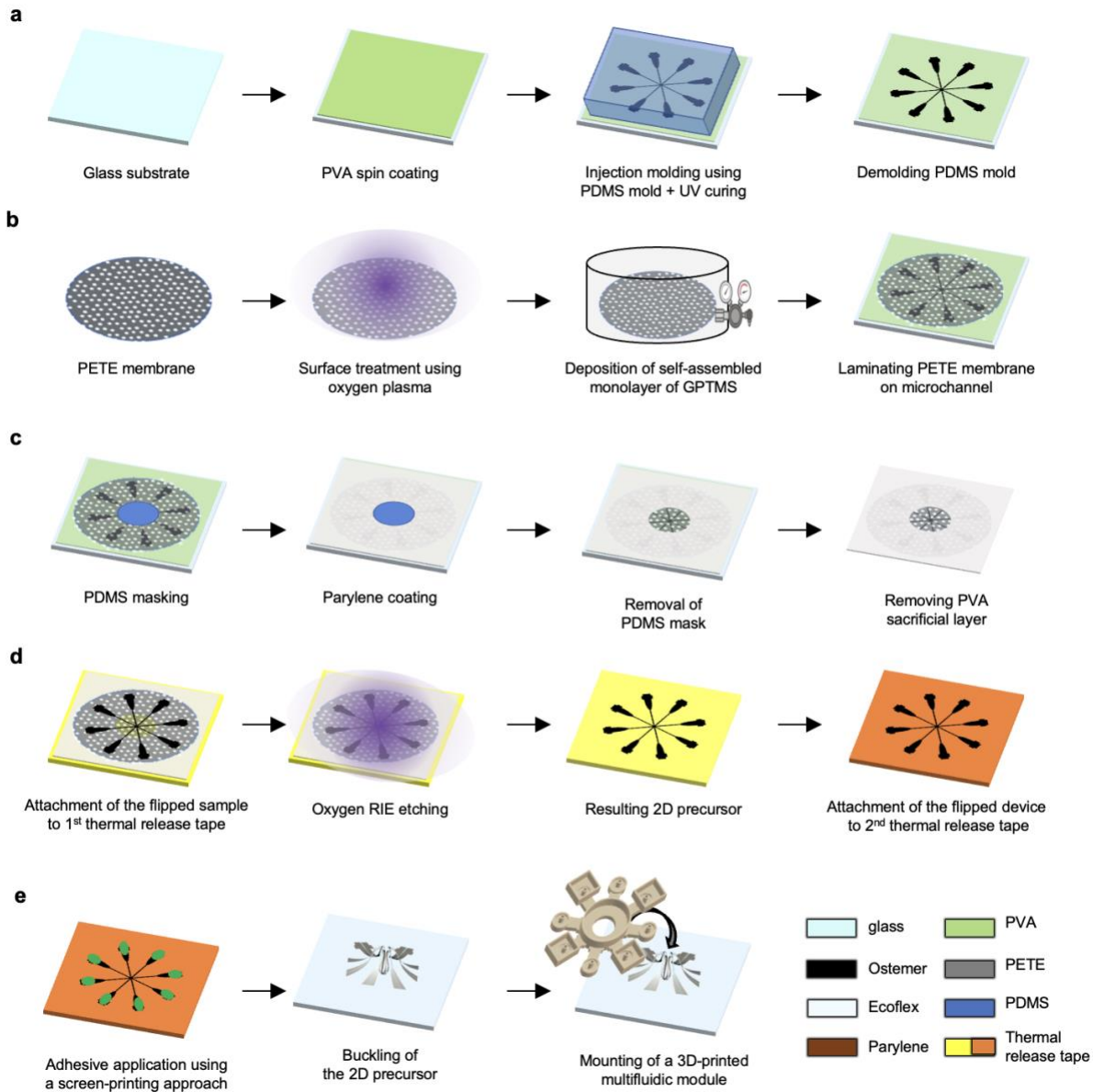
42 <sup>†</sup>These authors contributed equally

43 \* Corresponding Authors

45 Correspondence to [Juyeol Bae](#), [John A. Rogers](#) and [Colin K. Franz](#)

46

47	Supplementary Fig. 1   Fabrication processes for the multiscale 3D microfluidic platform. ....	3
48	Supplementary Fig. 2   Dimensional characteristics of the planar precursor.....	4
49	Supplementary Fig. 3   Mechanical characteristics of the material used for buckling the precursor 50 into 3D microchannel.....	5
51	Supplementary Fig. 4   A microfluidic device for multiplexed delivery of solutes at targeted 52 localized region.....	5
53	Supplementary Fig. 5   Top view of experimental setup for characterizing the mechanism of 54 solute transport through the porous interface into the agarose phantom. ....	6
55		
56	Supplementary Table 1   List of antibodies and molecular probes. ....	6
57		
58		



59

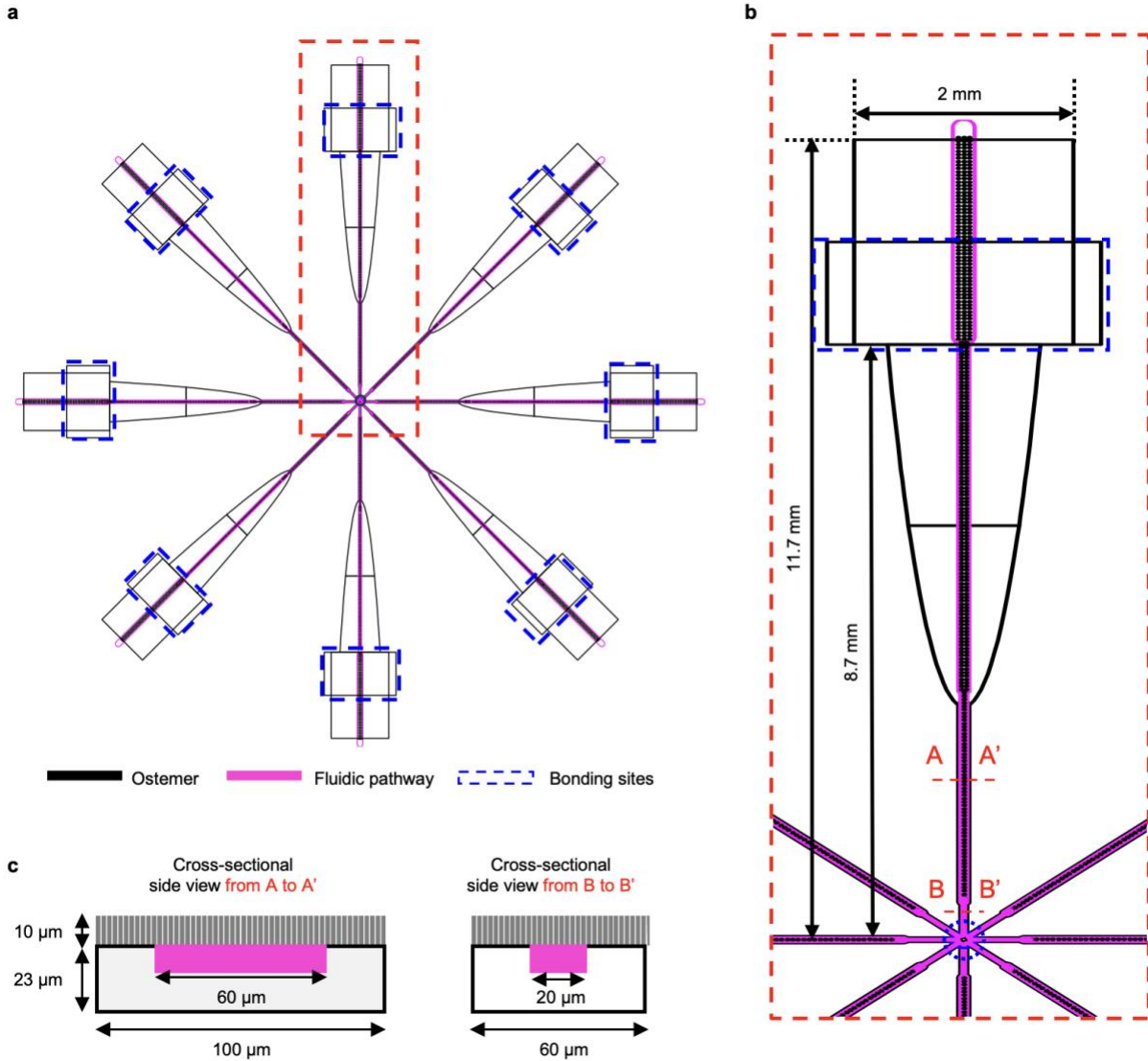
60 **Supplementary Fig. 1 | Fabrication processes for the multiscale 3D microfluidic platform.**

61 **a**, Soft-lithography step for preparing microchannel layer. **b**, Lamination step for bonding the  
 62 PETE membrane onto the prepared microchannel layer. **c**, Deposition step for selectively coating  
 63 parylene on the surface of the PETE membrane. **d**, Etching step for defining the PETE sheet into  
 64 the same 2D layout as the microchannel layer. **e**, Packaging step including buckling the 2D  
 65 precursor and mounting the 3D-printed millifluidic modules onto the periphery of the buckled 3D  
 66 microchannel.

67

68

69

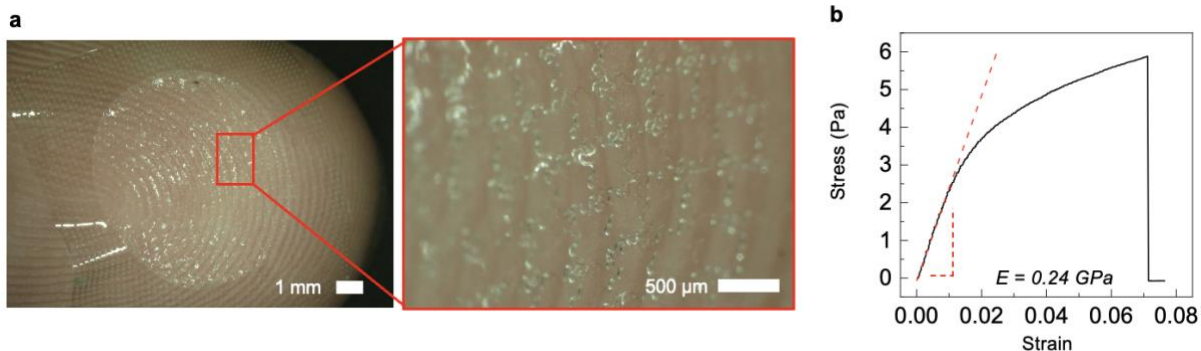


70

71 **Supplementary Fig. 2 | Dimensional characteristics of the planar precursor.**

72 **a**, 2D layout showing the design of the planar precursor. **b**, Enlarged view of a single wing in the  
 73 2D layout. **c**, Cross-sectional side views of the planar precursor along lines A–A' and B–B' in the  
 74 enlarged view of the wing.

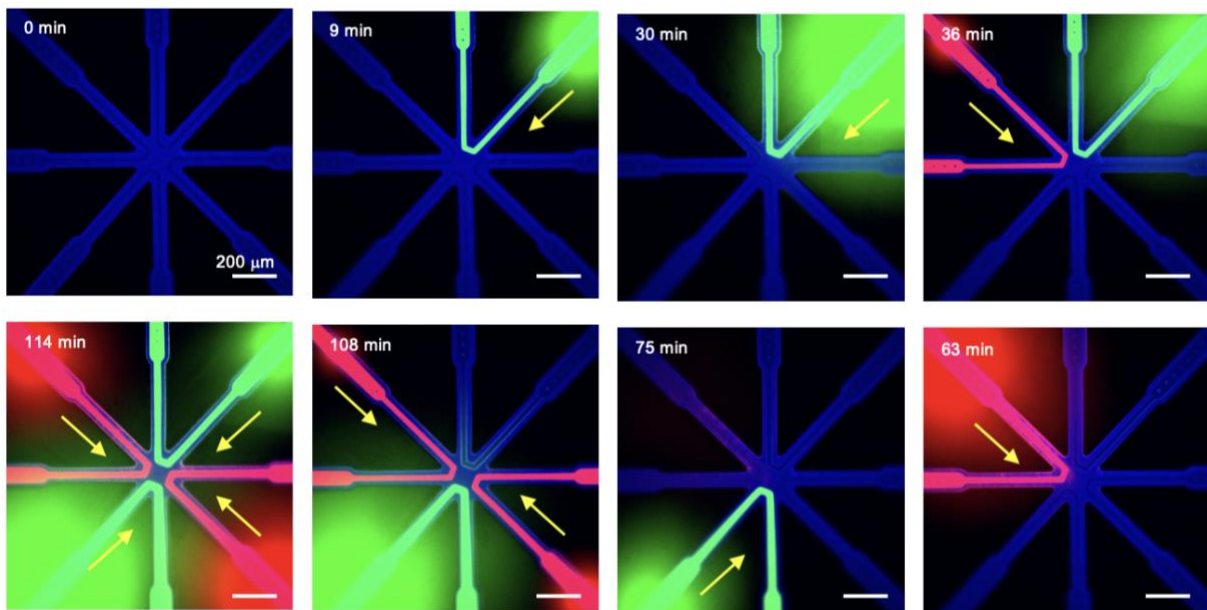
75



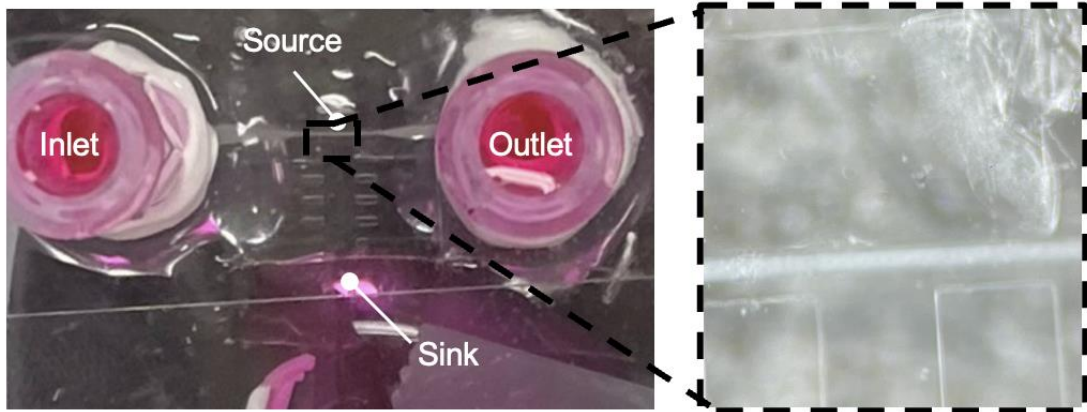
76  
77 **Supplementary Fig. 3 | Mechanical characteristics of the material used for buckling the**  
78 **precursor into 3D microchannel.**

79 **a**, Photographs showing an Ostemer microchannel layer placed on a fingerprint. The magnified  
80 view reveals that the layer conforms to the fingerprint ridges because the polymer is flexible  
81 (Young's modulus of  $10.29 \times 10^6 \text{ N/m}^2$ ). **b** Stress–strain curve obtained from tensile testing of the  
82 PETE membrane used to seal the microchannel layer.

83



84  
85 **Supplementary Fig. 4 | A microfluidic device for multiplexed delivery of solutes at targeted**  
86 Time-lapse widefield fluorescence microscopy showing multiplexed spatiotemporal delivery of  
87  $50 \mu\text{M}$  SRB and  $100 \mu\text{M}$  fluorescein isothiocyanate (FITC) into 2-mm-thick 1% agarose. Arrows  
88 indicate the flow direction of the solutions from the upstream wing.



89  
90  
91

**Supplementary Fig. 5 | Top view of experimental setup for characterizing the mechanism of solute transport through the porous interface into the agarose phantom.**

92

Antibody	Species	Dilution	Catalogue number, Company
Olig2	rabbit	1:100	AB9610, Millipore Sigma
Pax6	mouse	1:200	ab245110, abcam
Islet1	goat	1:2000	AF1837, Bio-Techne
NF Vio R667	human	1:1000	130-131-154, Miltenyi Biotec
NeuN Vio R667	human	1:1000	130-131-153, Miltenyi Biotec
Goat anti Mouse Alexa Fluor™ 555	mouse	1:1000	A-21424, Thermo Fisher Scientific
Donkey anti Rabbit Alexa Fluor™ 647	rabbit	1:1000	A-31573, Thermo Fisher Scientific
Donkey anti Rabbit Alexa Fluor™ 555	rabbit	1:1000	A-31572, Thermo Fisher Scientific
Donkey anti Goat Alexa Fluor™ 555	goat	1:1000	A-21432, Thermo Fisher Scientific
DAPI		1:50	D1306, Invitrogen
DRAQ5		1:100	ab108410, Abcam
Cholera Toxin Subunit B (Recombinant), Alexa Fluor™ 555 Conjugate		1:100	C22843, Invitrogen

93 **Supplementary Table 1 | List of antibodies and molecular probes.**